Journal of Sound and Vibration (1997) **200**(5), 605–620

MATHEMATICAL MODELLING OF A HELICOPTER ROTOR TRACK AND BALANCE: RESULTS

R. Ben-Ari and A. Rosen

Faculty of Aerospace Engineering, Technion—Israel Institute of Technology, Haifa, Israel

(*Received* 7 *January* 1996, *and in final form* 18 *July* 1996)

A mathematical model of a helicopter rotor track and balance is used in order to study optimal balancing and tracking, and their relationship. It is shown that perfect tracking does not necessarily lead to optimal balancing. Furthermore, cases of perfect tracking, may be accompanied by relatively high vibrations. Tracking or balancing at a certain air speed may also be accompanied by relatively large vibrational loads at other air speeds. Thus, it is recommended to perform simultaneous balancing at different air speeds. The present investigation shows how the new model can be used for optimal balancing of helicopter rotors.

1. INTRODUCTION

In the companion paper [1], a mathematical model of a helicopter rotor track and balance was presented. In this second paper the model will be used in order to investigate the tracking and balancing procedures and the differences between them.

The present numerical investigation will be concentrated on a typical four-bladed rotor, similar to that of the Apache AH-64. This rotor will be described in detail in section 2. In this section, the correction parameters (see reference [1]) that are used in order to minimize the influence of the natural (unintentional) non-uniformity will be presented.

In section 3, the various numerical aspects of the model will be presented and discussed. Verification of the model is presented in section 4.

In section 5, the tracking or balancing results are presented. First, tracking or balancing at a single air speed is described, and the behavior of the rotor at various air speeds is examined. Then, simultaneous balancing at two air speeds is studied and the results are compared with those for the same operation at a single air speed.

In section 6, the conclusions of the study are presented.

2. THE ROTOR MODEL

All of the numerical examples presented in what follows refer to a four-bladed ($b = 4$) rotor, similar to the Apache AH-64 rotor. The rotor has a radius of 7·76 m and rotates at an angular speed of $\Omega = 30$ rad/s. The offset of the rotor is 5·7%. The length of each blade is 7·32 m (see Figure 1), while the chord length is constant (along the blade) and equals 0·53 m. There are two stations along the blade at which balance weights can be added or subtracted, at distances of 0·63 m and 1·69 m from the root (see Figure 1). The root point O, is attached at a distance of $eR = 0{\cdot}44$ m from the

0022–460X/97/100605 + 16 $25.00/0/sv960670

hub center. Each blade has four trailing edge tabs. The length of each tab is 0·59 m (8% of the blade length), while the tab chord is 0·053 m (10% of the blade chord). The locations of the tabs are shown in Figure 1.

The nominal blade mass is $m_N = 76{\cdot}1$ kg. The nominal first mass moment about the flapping hinge is $K_N = 278{\cdot}6$ kg m. The nominal mass moment of inertia about the flapping hinge is $I_N = 1360$ kg m^2, while the nominal moment of inertia about the lead–lag hinge is larger by 1·34 kg m^2. The blade moment of inertia about the pitch axis is $I_P = 1{\cdot}34$ kg m^2. The non-principal components of the baled moment of inertia are small and thus assumed to be zero, except for I_{yz} (the blade co-ordinate system is used while calculating all these parameters—see Figure 3 of reference [1]) which is equal to 0·28 kg m^2. There is viscous damping at the lead–lag hinge, with a damping coefficient of $C_\zeta = 1000$ N m/(rad/s).

It is assumed that the air density equals 1·225 kg/m^3. A linear aerodynamic behavior of each cross-section is assumed, having a uniform lift curve slope along the blade, that is equal to 5·7 1/rad. The cross-sectional drag coefficient and moment coefficient are also constant along the blade, and equal to 0·0194 and 0·004, respectively. There is a linear pretwist along the blade (washout), with a total different of 9° between root and tip.

All of the above characteristics are the nominal ones. It is assumed that in the nominal case all of the four root pitch angles of the various blades are identical, the tab deflections are equal to zero, and the balance weights of all the blades are identical (the influences of which are included in the above indicated nominal data).

In the present investigation, the non-uniformity of the blades is introduced by four kinds of perturbations (that are referred to in reference [1] as "natural" perturbations), about the nominal values: (a) non-uniformity of the pitch angle at the blade root (relative to the nominal value), $\Delta\theta^D_{Rk}$ ($k = 0, 1, 2, 3$); (b) $\Delta\theta_{Sk}$ ($k = 0, \ldots, 3$) represent variations in the magnitude of the total built in twist (relative to the nominal value of 9°); (c) ΔK_k ($k = 0, \ldots, 3$) are variations in the blade first mass moment, about the flapping hinge; (d) ΔI_k ($k = 0, \ldots, 3$) are variations in the blade mass moment of inertia, about the flapping hinge. All these non-uniformities may be the result of manufacturing inaccuracies or imperfections that have developed during operation of the helicopter.

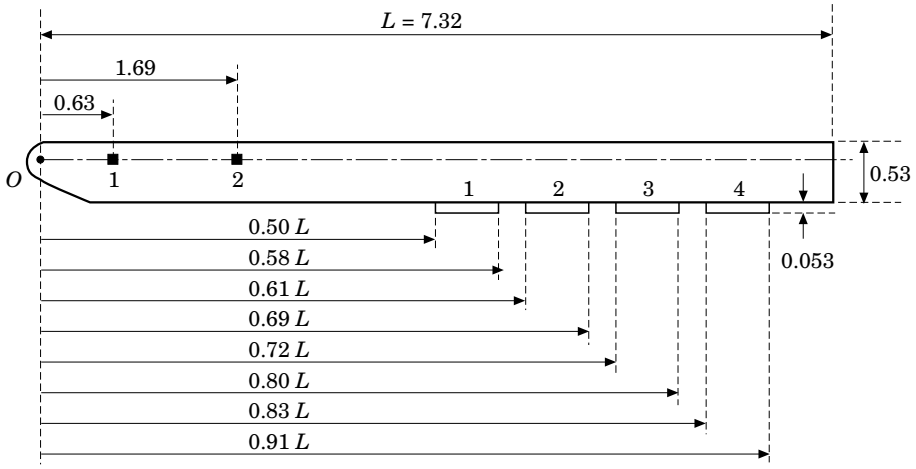

Figure 1. The geometry of the blade (all dimensions are in meters). ■, Balancing weight location.

The vector of natural perturbations of the kth blade (see equation (4.1) of reference [1]) is then

$$\mathbf{d}_k = \{\Delta\theta^D_{Rk}, \Delta\theta_{Sk}, \Delta K_k, \Delta I_k\}, \tag{2.1}$$

The vector of natural perturbations of the entire rotor (see equation (4.11) of reference [1]) is

$$\mathbf{d} = \{\mathbf{d}_0, \mathbf{d}_1, \mathbf{d}_2, \mathbf{d}_3\}, \tag{2.2}$$

where $\mathbf{d}$ is a vector of order 16.

The correction parameters of each blade include the following: (a) variation of the ptich rod setting—this variation results in a variation of the pitch angle at the blade root, $\Delta\theta^E_{Rk}$; (b) variation of the angle of the trailing edge tab—δ_{jk} is the angle of the jth tab of the kth blade; the inner tab is the first one ($j = 1$), while the tab number increases outward ($1 \leqslant j \leqslant 4$); the tab angle is measured relative to the direction of the cross-sectional zero lift line, and a positive angle indicates a downward deflection of the tab; (c) variation of the balance weights—m_{nk} is the variation in the mass of the balance weight that is located at the nth balance weight station of the kth blade, and in the present case (see Figure 1), $n = 1$ or 2.

There are certain constraints imposed on the magnitude of the variations of the correction parameters, as follows: (a) the variation in the length of the pitch link is limited such that

$$-2^\circ \leqslant \Delta\theta^E_{Rk} \leqslant 2^\circ; \tag{2.3}$$

(b) the bending of the trailing edge tabs is also limited, such that

$$-9^\circ \leqslant \delta_{jk} \leqslant 9^\circ; \tag{2.4}$$

Usually tabs that are bent too much tend to "bend back" during operation, due to their elasticity—the present analysis will not consider inaccuracies in the bending of the tabs, and thus it will be assumed that accurate determination of δ_{jk} is possible; (c) The magnitude of the variations in the balance weights is also limited, such that

$$-1 \text{ kg} \leqslant m_{nk} \leqslant 1 \text{ kg}; \tag{2.5}$$

in practice, variations of m_{nk} are not continuous and occur in steps—nevertheless, in the present analysis a continuous variation is allowed.

The vector of correction parameters of the kth blade (see equation (4.2) of reference [1]) is

$$\mathbf{e}_k = \{\Delta\theta^E_{Rk}, \delta_{1k}, \ldots, \delta_{4k}, m_{1k}, m_{2k}\}. \tag{2.6}$$

The vector of correction of parameters of the entire rotor (see equation (4.12) of reference [1]) is

$$\mathbf{e} = \{\mathbf{e}_0, \mathbf{e}_1, \mathbf{e}_2, \mathbf{e}_3\}. \tag{2.7}$$

3. THE NUMERICAL CALCULATIONS

As indicated by equation (5.8) of reference [1], the tracking problem is defined mathematically by the equation

$$\Delta\boldsymbol{\beta}^{CT} = \mathbf{S}^{\beta,E}\mathbf{e} + \mathbf{g}. \tag{3.1}$$

g is a vector that describes the natural tracking error due to the blades' non-uniformity. **e** is the vector of correction parameters (see equation (2.7)), while $\mathbf{S}^{\beta,E}$ is the sensitivity matrix of flapping, with respect to the correction parameters.

The purpose of the tracking procedure is to find vector **e**, which will result in the minimum absolute value of the vector of the tracking errors, $\Delta\boldsymbol{\beta}^{CT}$.

The vector **g** itself can be described in the following manner (see equation (5.9) of reference [1]):

$$\mathbf{g} = \mathbf{S}^{\beta,D}\mathbf{d} - \Delta\boldsymbol{\beta}_M^C. \tag{3.2}$$

Vector $\Delta\boldsymbol{\beta}_M^C$ describes the average tracking error (relative to the nominal blade), while $\mathbf{S}^{\beta,D}$ is the sensitivity matrix of flapping with respect to the natural perturbations.

The balancing problem is defined in a similar manner, as (see equation (5.10) of reference [1]):

$$\Delta\boldsymbol{\ell}^{CH} = \mathbf{S}^{LCH,E}\mathbf{e} + \mathbf{h}. \tag{3.3}$$

Here **h** is the vector of natural oscillatory loads due to the blades' natural non-uniformity, which are transferred from the rotor to the hub. $\mathbf{S}^{LCH,E}$ is the sensitivity matrix of the oscillatory loads, with respect to the correction parameters. $\Delta\boldsymbol{\ell}^{CH}$ is the vector of residual oscillatory loads. Optimal balancing is aimed at finding the vector **e** which will minimize the absolute value of $\Delta\boldsymbol{\ell}^{CH}$.

It is convenient to describe **h** as (see equation (5.11) of reference [1])

$$\mathbf{h} = \mathbf{S}^{LCH,D}\mathbf{d}, \tag{3.4}$$

where $\mathbf{S}^{LCH,D}$ is the sensitivity matrix of the oscillatory loads, with respect to the natural perturbations.

The four sensitivity matrices can be obtained by calculation, or on the basis of experimental measurements. For the present investigation these matrices are obtained by using a computer code that includes detailed rotor calculations, based on a blade-element approach. Mechanical couplings or direct aerodynamic couplings between the blades, are not taken into account. The present analysis includes only rigid motions of the blades and does not include elastic deformations. As indicated in reference [1], if elastic deformations are included, then $\Delta\boldsymbol{\beta}^{CT}$ refers to the tip path plane motion and reflects the resultant influences of rigid body flapping and elastic deformations. If necessary, more sophisticated aeroelastic comprehensive codes can be used to calculate the sensitivity matrix, including more complicated aerodynamic models. However, the current state-of-the-art in prediction of helicopter vibration is such that accurate results are in question. Therefore, it seems that obtaining the sensitivity matrices from flight tests, where controlled "intentional" known perturbations are introduced, is an attractive option.

The partial derivatives that define the elements of the matrices (see equations (4.6), (4.7), (4.14) and (4.15) of reference [1]) are calculated numerically, about the nominal state ($\mathbf{d} = \{0\}$, $\mathbf{e} = \{0\}$). The derivative of a certain variable f, with respect to x_j, according to the central difference scheme, is

$$\left(\frac{\partial f}{\partial x_j}\right)_{x_{jN}} = \frac{f(x_{jN} + h/2) - f(x_{jN} - h/2)}{h}. \tag{3.5}$$

All of the variables in the last equation obtain their nominal values, except for x_j (its nominal value is x_{jN}).

The magnitude of h is very crucial to the accuracy of the derivative calculation. An automatic test procedure of the convergence was used, in order to assure accurate calculations of the derivatives.

It should be emphasized that the sensitivity matrices are functions of air speed, weight and atmospheric conditions. The above-described procedure of calculating the sensitivity matrices is general and can easily be applied by using any computer code for calculating helicopter vibrations. Moreover, the same method of calculating the matrix elements can be followed by using flight test results. In this case a known perturbation is introduced before each flight and its influence on the vibrations is then measured.

4. VERIFICATION OF THE MODEL

Verification of the numerical model is based on introducing deterministic natural perturbations, and then calculating the optimal correction parameters that are needed in order to track or balance the rotor. The cases that will be described have solutions that can be determined based on simple physical reasoning. Thus, the numerical results can be verified.

4.1. VARIATION OF θ^D_{Rk} OF A CERTAIN BLADE

Pitch angle variations at the root of the blades are natural perturbations and also correction parameters. Thus, if the perturbation is $\Delta\theta^D_{R0} = 1^\circ$, then the optimal correction, that will lead to perfect tracking (that is, performed relative to the average natural tracking error), is $\Delta\theta^E_{R0} = -0{\cdot}75^\circ$ and $\Delta\theta^E_{R1} = \Delta\theta^E_{R2} = \Delta\theta^E_{R3} = 0{\cdot}25^\circ$. On the other hand, according to the present definitions, the correction that will lead to perfect balance is $\Delta\theta^E_{R0} = -1^\circ$ and $\Delta\theta^E_{R2} = \Delta\theta^E_{R3} = 0^\circ$. The calculations gave the same results.

4.2. PERTURBATIONS OF K_k AND I_k

It is always possible to find two balance weights, m_{1k} and m_{2k}, that cancel any pair of natural perturbations ΔK_k and ΔI_k. The numerical model gave results identical to those of direct calculations for these two masses.

4.3. IDENTICAL NATURAL PERTURBATIONS IN ALL THE BLADES

If the natural perturbations in all the blades are identical, then the blades remain identical. In such a case all the blades are in track and so tracking corrections are not required. In the case of balancing, where the corrections try to make the blades as similar as possible to the nominal one, the corrections in all the blades will be identical. The calculated results confirm these logical predictions.

5. NUMERICAL RESULTS

5.1. THE INPUT DATA AND METHOD OF PRESENTING THE RESULTS

Balancing or tracking takes place in a trimmed level flight. As indicated above, the sensitivity matrices are functions of the air speed, helicopter weight (and c.g. location) and atmospheric conditions. All the results presented here, are calculated for standard sea level atomospheric conditions, at a rotor thrust of 65 000 N. The trim position was calculated by using the method of reference [2], based on the Apache AH-64 data.

TABLE 1

The natural perturbations of the four blades

	$k=0$	$k=1$	$k=2$	$k=3$
$\Delta\theta^{D}_{Rk}$(degrees)	0·285	−1·415	1·344	−1·380
$\Delta\theta_{Sk}$(degrees)	−0·645	0·0765	0·422	−0·320
ΔK_k(kg m)	−0·062	−0·146	−0·030	0·194
ΔI_k(kg m^2)	0·786	0·030	0·078	0·160

Instead of referring to an air speed, we will refer to its non-dimensional equivalent, the advance ratio, μ, where

$$\mu \simeq \text{air speed}/(\text{tip speed}). \tag{5.1}$$

The natural non-uniformity of the rotor is defined by the vector **d** (see equation (2.2)). In the present case the terms of this vector have been determined by using a random procedure, while taking care that the elements stay within reasonable limits. The vectors $\mathbf{d}_k$ of all of the blades, used in all the following examples, are presented in Table 1.

The investigation starts by balancing or tracking the rotor at a single air speed.

If balancing is considered, then μ_B indicates the advance ratio at which this balancing takes place, Thus, the vector of correction parameters **e**, that minimizes the absolute value of $\Delta\ell^{CH}$ at the advance ratio μ_B is calculated. In order to check how vector **e** affects the vibrational loads or tracking at an advance ratio μ_F, equation (3.1) or (3.3) is used, where the sensitivity matrices are calculated at μ_F. If $\mu_F = \mu_B$, then the optimal case is considered. Nevertheless, it is very important and interesting to investigate cases in which $\mu_F \neq \mu_B$.

If tracking is considered, then μ_T defines the advance ratio at which vector **e** minimizes tha aboslute value of $\Delta\boldsymbol{\beta}^{CT}$. Again, one should be interested in checking how vector **e** affects the vibrational loads or tracking at an advance ratio μ_F.

In order to present a measure of the intensity of the vibrational forces, associated with certain harmonic, a norm of the loads at frequency $i\Omega$, $\Delta F^{H,i}$, is defined as follows (see equations (3.7) and (3.10) of reference [1]):

$$\Delta F^{H,i} = [(\Delta F_x^{HiS})^2+(\Delta F_x^{HiC})^2+(\Delta F_y^{HiS})^2+(\Delta F_y^{HiC})^2+(\Delta F_z^{HiS})^2+(\Delta F_z^{HiC})^2]^{1/2}. \tag{5.2}$$

In similar manner, in order to measure the intensity of the vibrational moments, a moment norm, $\Delta M^{H,i}$, is defined:

$$\Delta M^{H,i} = [(\Delta M_x^{HiS})^2+(\Delta M_x^{HiC})^2+(\Delta M_y^{HiS})^2+(\Delta M_y^{HiC})^2]^{1/2}. \tag{5.3}$$

The index i in equations (5.2) and (5.3) takes on (in general) the values $i = 1, \ldots, 5$. The zeroth component ($i = 0$) does not affect the vibrations and thus is of no interest here.

In order to assess the tracking quality at frequency $i\Omega$, the norm $\Delta\beta^i$ is defined:

$$\Delta\beta^i = \left\{\sum_{k=0}^{b-1}\left[(\Delta\beta_k^{CT,iS})^2+(\Delta\beta_k^{CT,iC})^2\right]\right\}^{1/2}. \tag{5.4}$$

$\Delta\beta_k^{CT,iS}$ and $\Delta\beta_k^{CT,iC}$ are the elements of the vector $\Delta\boldsymbol{\beta}_k^{CT}$, that refer to the sine and cosine components, respectively, of the ith harmonic of the flapping of the kth blade. In equation (5.4), i takes on values between zero and five. According to the present definitions, in the case of tracking, the components $i = 0$ are also important.

The above discussion dealt with balancing or tracking at a certain advance ratio, as well as measuring its effects at various advance ratios. Since the present formulation is based

on a least squares approach, that deals with overdetermined systems of equations, extension of the balancing or tracking procedure to multiple air speeds is straightforward. It leads to a simultaneous solution of the balancing or tracking equations at various air speeds (see examples below).

5.2. BALANCING OR TRACKING AT A SINGLE AIRSPEED

In this section balance versus tracking, at a single air speed, will be investigated. The natural perturbations are those that are presented in Table 1.

In order to allow some insight into the problem, a relatively simple case will be studied. The correction parameters in the examples presented are confined to three for each blade: (a) the pitch and angle at the root, $\Delta\theta^E_{Rk}$; (b) the deflection angle of tab number 4, δ_{4k}; (c) the balancing weight at station number 1, m_{1k}. Thus, the correction vector of the rotor ($b = 4$), **e**, is of order 12.

The calculations show that the vibrations (because of non-uniformity), at frequencies 4Ω and 5Ω, are very small and thus can be neglected. The present investigation will be concentrated on the low frequencies (Ω, 2Ω, 3Ω). Vibrations at these frequencies are solely due to non-uniformity and do not appear in the case of a four-bladed rotor with uniform blades. After neglecting the higher frequencies, the problem of balancing at a single air speed, is associated with 35 equations (three force components and two moment components—for each one there is a constant term and three sine and cosine harmonics). With 12 variables (the dimension of vector **e**), an overdetermined system is obtained.

5.2.1. *Balancing or tracking at hover* ($\mu_B = \mu_T = 0$)

At first, balancing or tracking at hover are considered, namely $\mu_B = \mu_T = 0$. The vectors **e** for balancing or tracking are presented in the first and fourth columns of Table 2, respectively.

In Figures 2(a)–(c), the influence of balancing or tracking at hover, on the behavior at hover ($\mu_F = 0$) is presented. The norms $\Delta\beta^i$ before and after balancing or tracking, are presented in Figure 2(a): (a) OR refers to the original case of natural perturbations, when $\mathbf{e} = \{0\}$; (b) AB indicates results after balancing; (c) AT indicates results after tracking.

TABLE 2

The correction parameters of balancing or tracking

	μ_B			μ_T	
$\{E\}$	0	0·25	0, 0·25	0	0·25
$\Delta\theta^E_{R0}$(degrees)	−0·56	−0·54	−0·54	−0·83	−0·82
δ_{40}(degrees)	−2·95	−3·10	−3·10	−2·02	−2·13
m_{10}(g)	70	397	314	135	−400
$\Delta\theta^E_{R1}$(degrees)	1·45	1·45	1·45	1·21	1·21
δ_{41}(degrees)	0·38	0·26	0·26	0·76	0·79
m_{11}(g)	255	416	333	197	391
$\Delta\theta^E_{R2}$(degrees)	−1·17	−1·18	−1·17	−1·40	−1·40
δ_{43}(degrees)	1·96	2·07	1·99	2·19	2·28
m_{12}(g)	31	330	259	−11	520
$\Delta\theta^E_{R3}$(degrees)	1·25	1·25	1·25	1·0	1·0
δ_{43}(degrees)	−1·49	−1·46	−1·52	−0·94	−0·94
m_{13}(g)	−284	149	−221	−321	−511

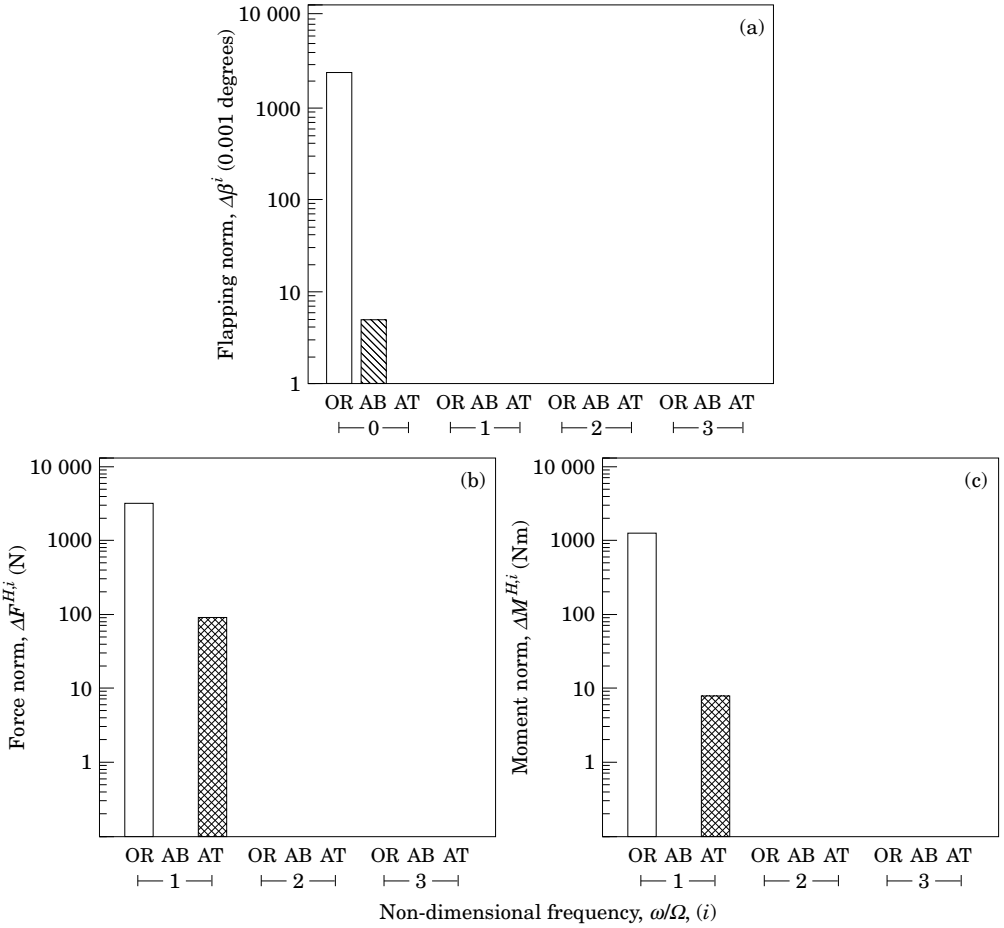

Figure 2. Balancing or tracking at hover ($\mu_B = \mu_T = 0$). (a) Tracking norms at hover ($\mu_F = 0$); (b) force norms at hover ($\mu_F = 0$); (c) moment norms at hover ($\mu_F = 0$). OR, original; AB, after balancing; AT, after tracking.

Since the differences in the levels of the norms range over a few orders of magnitude, a half logarithmic scale is used.

It can be seen that there is a relatively large flapping deviation at the basic state (OR), of the order of 2·5°. Tracking leads to a (practically) zero tracking error. Balancing (AB) leaves a very small tracking error (less than 0·01°) that is practically negligible. With the present equipment, the ground crew can detect tracking errors of the order of a few hundredths of a degree.

The force norms of the various harmonics, $\Delta F^{H,i}$, are presented in Figure 2(b). The original state presents a fairly large amplitude, close to 3000 N. Balancing practically cancels the vibrational forces due to non-uniformity. Tracking, on the other hand, that leads to a zero tracking error, leaves vibrational forces having an amplitude close to 100 N. This means a significant reduction in the vibrations, relative to the original state, but still much larger vibrations than those that are obtained after balancing.

The vibrational moments, presented in Figure 2(c), exhibit a behavior that is similar to that of the forces in Figure 2(b).

In Figures 3(a)–(c) the tracking and load norms are presented for forward flight ($\mu_F = 0{\cdot}25$), after balancing or tracking at hover ($\mu_B = \mu_T = 0$). As expected, in forward

flight there are original vibrations at all the frequencies, unlike the case of hovering, in which the tracking errors included only zero frequencies and the load norms included only the first harmonic.

The tracking errors are presented in Figure 3(a). The amplitude of the norms of the original zero and first harmonics, are of the same order of magnitude as in hover, but the amplitudes decrease at higher frequencies. Tracking results in a zero tracking error, while balancing leaves a negligible tracking error at zero frequency.

The force norms are shown in Figure 3(b). Balancing in hover results in small vibrational forces (~ 5 N) at a frequency of Ω, while tracking in hover results in a larger force norm (~ 100 N at that frequency). The same behavior is also shown at a frequency of 2Ω, but the amplitude of the norms decreases and so does the difference between them. The force norms at a frequency of 3Ω are the smallest, with the force norm after balancing somewhat larger than that after tracking. This behavior at a frequency of 3Ω, does not change the observation that balancing results in smaller vibrations than does tracking, since the vibrations at 3Ω are much weaker than the vibrations at Ω and 2Ω.

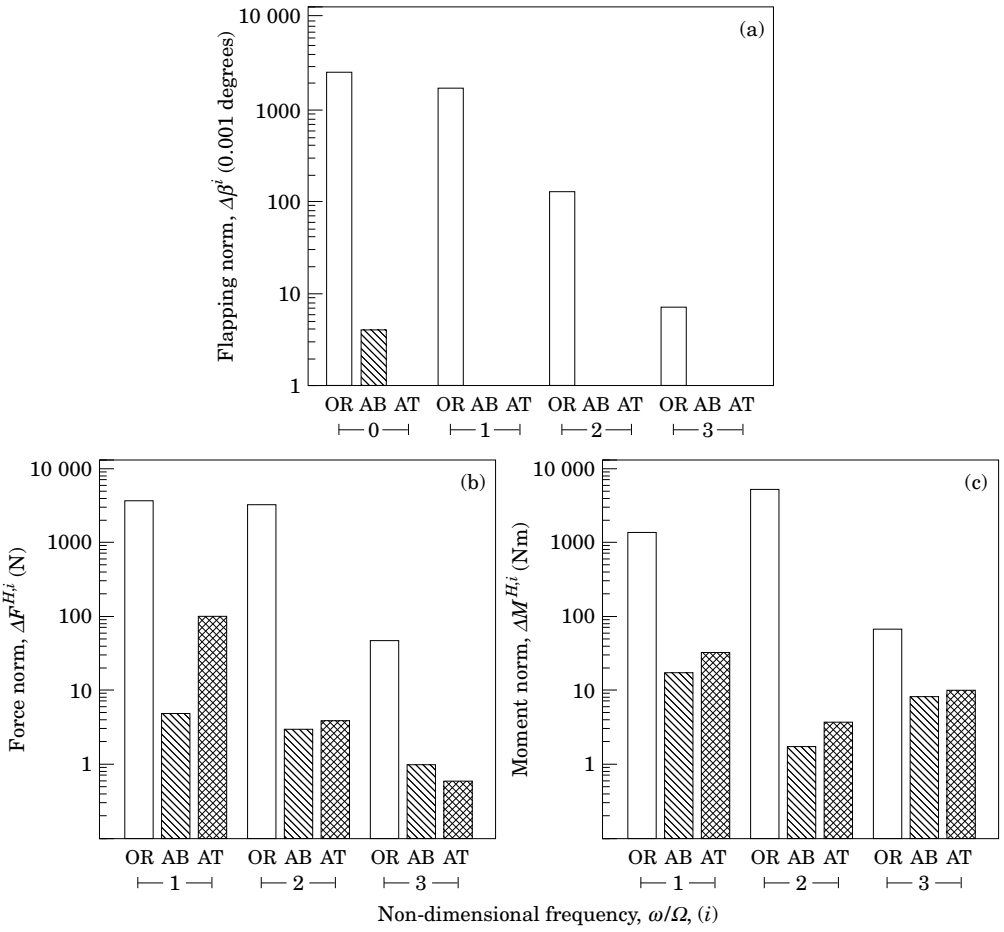

Figure 3. Balancing or tracking at hover ($\mu_B = \mu_T = 0$). (a) Tracking norms at forward flight ($\mu_F = 0{\cdot}25$); (b) force norms at forward flight ($\mu_F = 0{\cdot}25$); (c) moment norms at forward flight ($\mu_F = 0{\cdot}25$). OR, original; AB after balancing; AT, after tracking.

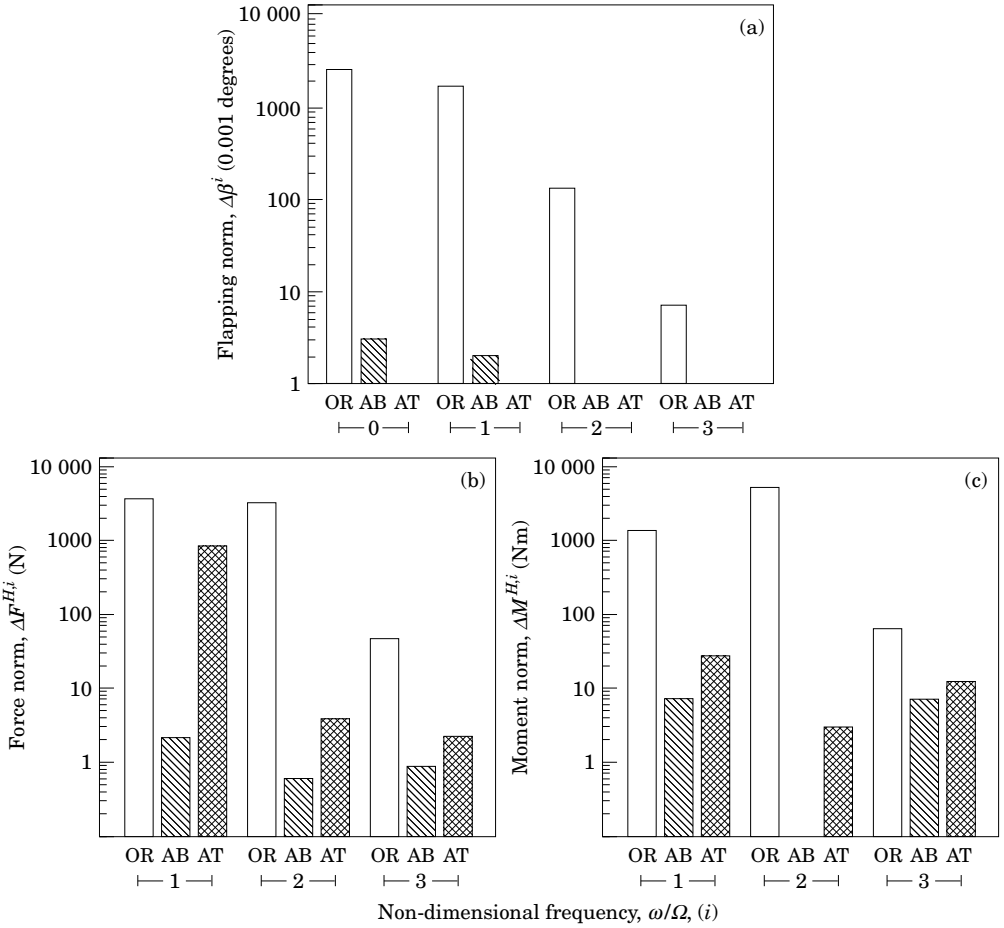

Figure 4. Balancing or tracking at forward flight ($\mu_B = \mu_T = 0.25$). (a) Tracking norms at forward flight ($\mu_F = 0{\cdot}25$); (b) force norms at forward flight ($\mu_F = 0{\cdot}25$); (c) moment norms at forward flight ($\mu_F = 0{\cdot}25$). OR, original; AB after balancing; AT, after tracking.

The results for the moment norms are shown in Figure 3(c). The trends are similar to those of the force norms, except for the fact that relative differences between the norms (after balancing or tracking) are smaller.

5.2.2 *Balancing or tracking at forward flight* ($\mu_B = \mu_T = 0{\cdot}25$)

The influences of balancing or tracking at forward flight ($\mu_F = 0{\cdot}25$), are presented in Figures 4(a)–(c). The vectors **e** for balancing and tracking are presented in the second and fifth columns of Table 2, respectively. In Figure 4(a) it is shown again that tracking results in a zero tracking error at the same air speed, while balancing leaves a very small tracking error. The difference between balancing and tracking, when it comes to the vibrational loads, is presented very clearly in Figure 4(b). In the case of the first frequency, Ω, the norm of the force after tracking is larger by almost three orders of magnitude compared to the force norm after balancing (900 N as compared to 2 N). It is shown that perfect tracking will still leave place for significant vibrations of the fuselage ($\sim 0{\cdot}01$ g). In the case of the moment norms, the trend is similar to that of the force norms, but the differences between the results after balancing or tracking are much smaller.

The influences of balancing or tracking at forward flight ($\mu_B = \mu_T = 0{\cdot}25$), on the tracking errors or vibrations at hover, are shown in Figures 5(a)–(c). It is shown that tracking at forward flight also results in perfect tracking at hover (Figure 5(a)), but it is accompanied by large vibrational forces (Figure 5(b)), having a norm of 900 N. This force norm is larger by two orders of magnitude than the force norm that is obtained in hover, after balancing in forward flight. At first sight it may seem that the moment norms (Figure 5(c)) exhibit an opposite trend, with the moment norm after balancing somewhat larger than the one after tracking. This "opposite trend" is understandable, if one recalls that balancing means finding the minimum absolute value of the loads vector (see equation (3.3)), which includes both force and moment components. Since the weights of all the components are identical, the importance of the moment components, relative to the force components, is small, since the force components are larger. If necessary, different weights can be given to different equations.

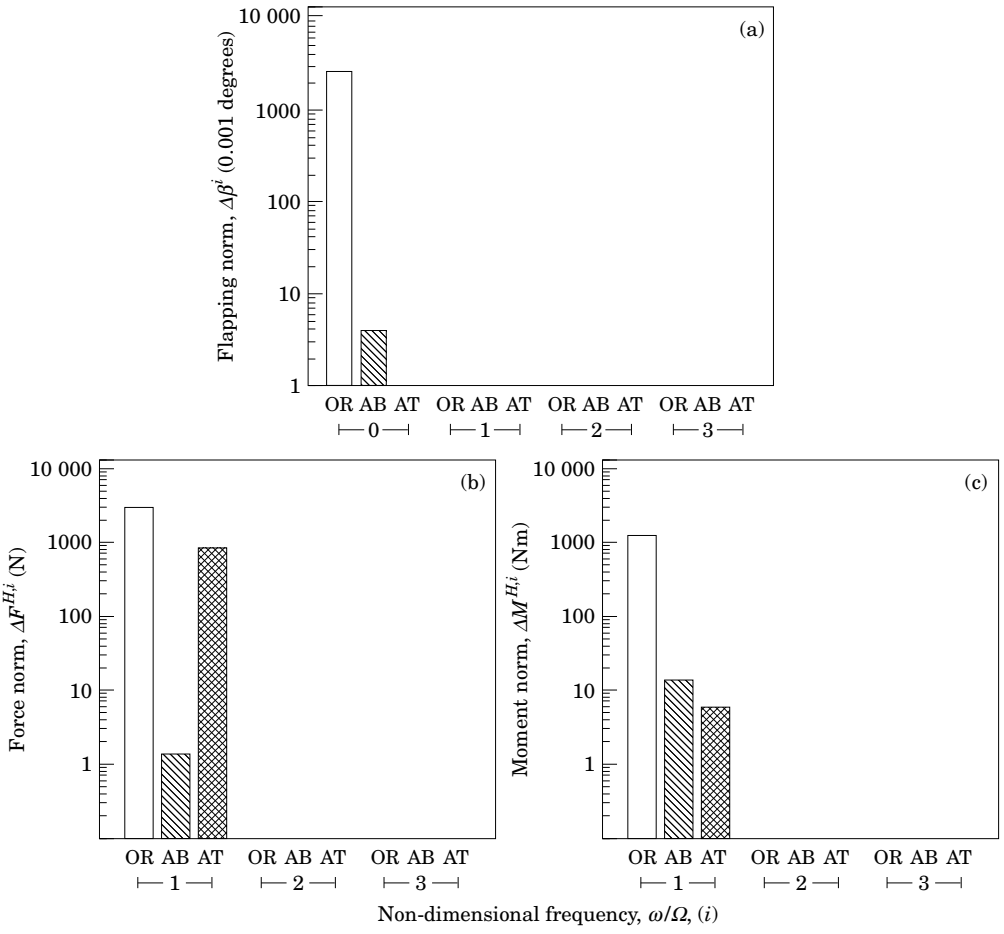

Figure 5. Balancing or tracking at forward flight ($\mu_B = \mu_T = 0{\cdot}25$). (a) Tracking norms at hover ($\mu_F = 0$); (b) force norms at hover ($\mu_F = 0$); (c) moment norms at hover ($\mu_F = 0$). OR, original; AB after balancing; AT, after tracking.

5.2.3. *Summary of results for balancing or tracking at a single air speed*

The investigation presented above was also repeated for another random set of natural perturbations. Results and trends identical to those presented above were observed. On the basis of all of the results, the following conclusions can be drawn.

(a) In all of the cases investigated, tracking in hover or forward flight resulted in a decrease in the magnitude of the vibrational loads. Nevertheless, the magnitude of the vibrational loads after tracking was higher, sometimes significantly, than the same loads after balancing.

(b) In Figure 3(b) it is shown that tracking in hover results in force norms of the order of 100 N at a frequency of Ω, in forward flight. In Figure 4(b) it is shown that tracking in the same forward flight results in much higher force norms (800 N for frequency Ω). The force and moment norms at the other frequencies show a similar trend, while comparing both cases. It should be noted that tracking in hover also results in perfect tracking in forward flight. Thus, it turns out that two perfect tracking procedures lead to two significantly different levels of vibrations, at the same air speed.

(c) Examination of the results in Table 2 indicates that the correction of the root pitch angle $\Delta\theta_{Rk}^{E}$ and the deflection of the tab δ_{4k}, for any k, are almost identical as a result of balancing at hover or forward flight. The same also applies for tracking. The relative differences in these parameters, as a result of balancing (or tracking) at two different air speeds, usually do not exceed 4% in the case of $\Delta\theta_{Rk}^{E}$, and 10% in the case of δ_{4k}. On the other hand, the differences in the balance weights m_{1k} that are obtained for different air speeds are very large, and usually reach 100%. Thus, it can be concluded that variations in $\Delta\theta_{Rk}^{E}$ and δ_{4k} are very effective and can be considered as the basic corrections of the non-uniformity. The balance weights are used for "secondary" fine tuning. This fine tuning (by m_{1k}) exhibits the major differences between balancing or tracking at various air speeds.

5.3. SIMULTANEOUS BALANCING AT MULTIPLE AIR-SPEEDS

Usually, a helicopter operator is interested in balancing his rotor over a wide range of air speeds. The results of the previous section indicate that optimal balancing at a certain airspeed is not necessarily optimal at a different air speed. This raises the importance of simultaneous balancing at multiple air speeds. As explained previously, the present mathematical model, based on using a least squares method, allows easy extension of the model to include balancing or tracking at different air speeds. It simply results in an increase in the number of equations, without changing the dimensions of vectors **d** and **e**. By changing the weights of the equations at various air speeds, the relative importance of various air speeds can be varied.

As indicated above, in the present investigation the fourth and fifth harmonics are ignored. Thus, while balancing at a single air speed means a system of 35 equations, balancing at two different air speeds means the least squares solution of 70 equations. The number of correction parameters remains 12. The two advance ratios at which balancing will be carried out simultaneously are $\mu_B = 0$ and 0·25 (the same advance ratios that were investigated in the previous sections). The vibrational loads and tracking errors will also be presented at these two advance ratios ($\mu_F = 0$, $\mu_F = 0{\cdot}25$).

The correction parameters for balancing are presented in the third column of Table 2.

In Figure 6(a) and (b) the force and moment norms, respectively, of the various harmonics at hover ($\mu_F = 0$) are presented. The original norm is compared with balancing at hover only (a, $\mu_B = 0$), balancing at forward flight (b, $\mu_B = 0{\cdot}25$) and balancing at these two air speeds simultaneously (c, $\mu_B = 0, 0{\cdot}25$). Naturally, the best balancing (practically

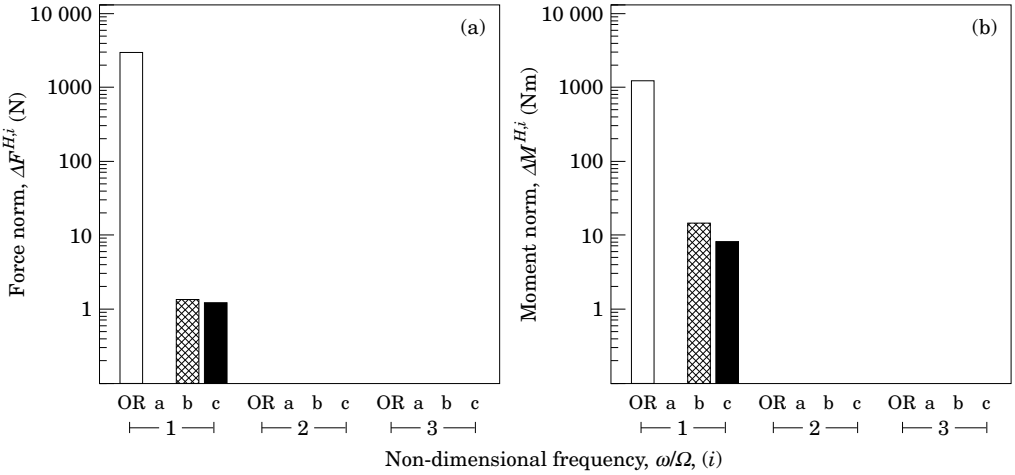

Figure 6. Combined balancing at two air speeds ($\mu_B = 0$, 0·25). (a) Force norms at hover ($\mu_F = 0$); (b) moment norms at hover ($\mu_F = 0$). OR, original; a, $\mu_B = 0$; b, $\mu_B = 0{\cdot}25$; c, $\mu_B = 0$, 0·25.

perfect) is obtained in the case of balancing at hover only. Small vibrational loads are obtained in cases b and c, having similar norms, with slightly higher value for b.

The force and moment norms in forward flight are presented in Figures 7(a) and (b), respectively. As expected, the best results are obtained when balancing is performed at the same air speed, in case b. Similar to the trends in Figures 6(a) and (b), balancing at the two air speeds c gives slightly higher vibrational loads. The strongest vibrations are obtained in the case of balancing at hover a.

In order quantitatively to compare the three balancing schemes, other norms of the vibrational loads, which sum up the contributions of the various harmonics, are defined:

$$\Delta \mathring{F}^{NR} = \left[\sum_{i=1}^{3} (\Delta F^{H,i})^2\right]^{1/2}, \qquad \Delta \mathring{M}^{NR} = \left[\sum_{i=1}^{3} (\Delta M^{H,i})^2\right]^{1/2}. \tag{5.5, 5.6}$$

The values for the present case are shown in Table 3.

It is shown in Figures 6 and 7, and in Table 3, that dual balancing presents a "compromise" between the separate balancings at $\mu_B = 0$ or $\mu_B = 0{\cdot}25$. Since the vibrations at forward flight are higher than the vibrations at hover, the results of the dual balancing $\mu_B = 0$, 0·25 resemble much more the results of $\mu_B = 0{\cdot}25$.

The tracking errors of the three balancing procedures are shown in Figure 8(a) for hover, and in Figure 8(b) for forward flight. All the procedures lead to very small tracking errors (less than 0·05°).

TABLE 3

A comparison between the resultant norms of the vibrational forces and moments at hover and forward flight, for various balancing procedures

$\mu_F =$	0			0·25		
$\mu_B =$	0	0·25	0, 0·25	0	0·25	0, 0·25
$\Delta \mathring{F}^{NR}$(N)	0	1·39	1·25	5·92	2·44	3·10
$\Delta \mathring{M}^{NR}$(N m)	0	13·80	8·07	19·40	10·30	12·20

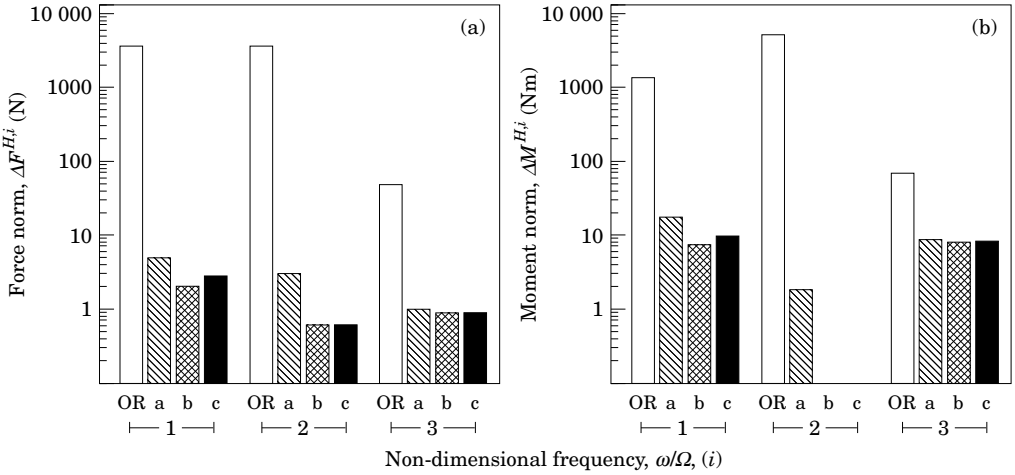

Figure 7. Combined balancing at two air speeds ($\mu_B = 0, 0{\cdot}25$). (a) Force norms at forward flight ($\mu_F = 0{\cdot}25$); (b) moment norms at forward flight ($\mu_F = 0{\cdot}25$). OR, original; a, $\mu_B = 0$; b, $\mu_B = 0{\cdot}25$; c, $\mu_B = 0, 0{\cdot}25$.

Results for simultaneous balancing at three advance ratios ($\mu_B = 0, 0{\cdot}2, 0{\cdot}3$) were obtained and studied, but are not presented here. The results were similar to those for dual balancing. The important conclusions are as follows:

(a) In all of the advance ratios that were examined (μ_F), balancing at multiple air speeds never led to maximum vibrations at any of these air speeds. Maximum vibrations always occur in the case of balancing at a single advance ratio, which differs significantly from μ_F.

(b) The correction parameters of balancing at various air speeds are always closer to a single air speed balancing at higher speeds, because the vibrations increase as the forward speed increases.

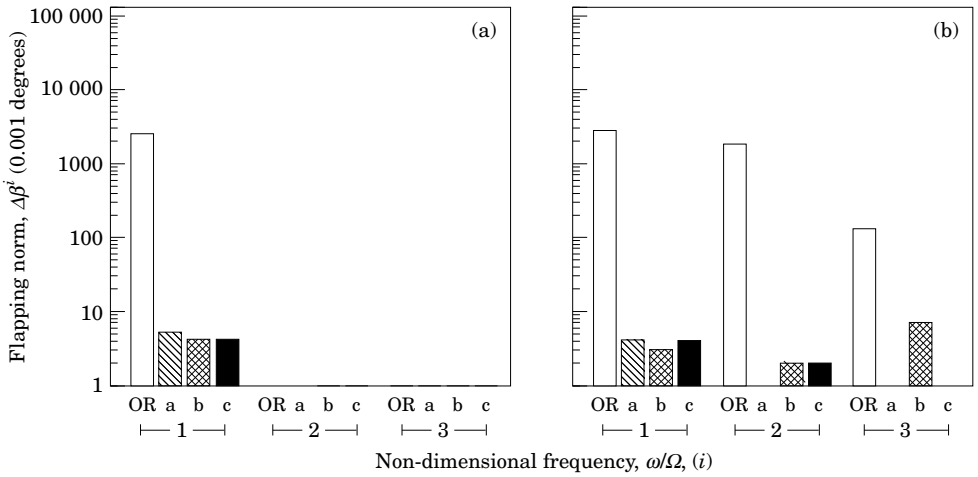

Figure 8. Combined balancing at two air-speeds ($\mu_B = 0, 0{\cdot}25$). (a) Tracking norms at hover ($\mu_F = 0$); (b) tracking norms at forward flight ($\mu_F = 0{\cdot}25$).

6. CONCLUSIONS

A mathematical model of balancing and tracking, has been used in this paper in order to study the success of these two procedures in decreasing the effects of non-uniformity between the helicopter rotor blades.

It has been shown that tracking leads to negligible tracking errors, in hover or in forward flight, while it also reduces the magnitude of the vibrational loads that are transferred from the rotor to the fuselage. Nevertheless, the magnitude of the vibrational loads after tracking is usually higher—sometimes significantly higher—than the loads that are transferred from the rotor to the hub after balancing.

The results indicate that "perfect" tracking may be obtained by using various combinations of correction parameters. However, while there are negligible differences between the tracking errors in these cases, they may be associated with relatively large differences in the vibrational loads that are transferred from the rotor to the helicopter fuselage.

The vibrational loads or tracking errors may be very sensitve to certain correction parameters. This means that small variations of these correction parameters have relatively large influences. It is shown that the variations in the values of these parameters, as obtained while balancing or tracking at different air speeds, are relatively small. On the other hand, if correction parameters that are less effective are considered, they may show relatively large differences in their values, which are obtained during balancing or tracking at different air speeds. It seems as if the more effective correction parameters are used for a coarse tuning, while the less effective ones are used for the fine tuning.

Usually, a helicopter operator is interested in balancing his rotor over a wide range of air speeds. The present least squares approach can be extended very easily to address cases of simultaneous balancing (or tracking) at multiple air speeds. In the present paper, results for balancing at dual air speeds are presented. The investigation also included results for three air speeds (that are not presented here, but showed similar trends).

The results indicated that simultaneous balancing at various air speeds results in a certain "averaging" between the correction parameters that are obtained after "individual" balancing at each of these air speeds. The results of balancing at various air speeds never gave the highest vibrations in any of those air speeds. The maximum vibrations are obtained when using the optimal balancing correction parameters at another (significantly different) air speed.

If the weights of the equations of balancing at different air speeds are identical, then the correction parameters that are obtained from "multiple" air speed balancing are closer to the results that are obtained from balancing at a single high air speed. This trend is due to the fact that the amplitude of the vibrational forces due to non-uniformity increases as the air speed is increased.

The important conclusion is that in order to optimize the rotor tuning, balancing should be preferred to tracking. In order to perform correct balancing, one should use the sensitivity matrices that were defined in this research. The sensitivity matrices should be known for different combinations of weights, atmospheric conditions and air speeds. The present least squares approach is very useful and convenient, since it allows simultaneous balancing (and also tracking) at different air speeds.

The theoretical model that was used in the present analysis in order to calculate the sensitivity matrices is relatively simple. It does not include elastic deformations and the aerodynamic model is fairly simple. However, this model was sufficient in order to carry out the investigation and present the comparison between balancing and tracking. If necessary, more sophisticated comprehensive aeroelastic models can be used. In such a

case, instead of flapping, the tip path plane should be considered, including the coupled influences of rigid flapping and elastic deformations. Furthermore, the current state-of-the-art in helicopter vibration prediction is often not sufficiently accurate. Therefore, it may be preferable to obtain the sensitivity matrices from flight tests, where known perturbations can be introduced in order to define the elements of the sensitivity matrices, at various flight conditions.

ACKNOWLEDGMENTS

This research was supported by the Fund for the Promotion of Research at the Technion.

REFERENCES

1. A. Rosen and R. Ben-Ari 1997 *Journal of Sound and Vibration* **200**, 589–603. Mathematical modelling of helicopter rotor track and balance: theory.
2. M. Chaimovich, A. Rosen and O. Rand 1993 *The Aeronautical Journal of the Royal Aeronautical Society* **97**, 14–24. A generic harmonic rotor model for helicopter flight simulation.